

XMM-NEWTON OBSERVATIONS OF OPTICALLY SELECTED SDSS CLUSTERS

M. PLIONIS^{1,2}, S. BASILAKOS¹, I. GEORGANTOPOULOS¹, A. GEORGAKAKIS¹

¹Institute of Astronomy & Astrophysics, National Observatory of Athens, I.Metaxa & B.Pavlou, P.Penteli
 152 36, Athens, Greece

² Instituto Nacional de Astrofisica, Optica y Electronica (INAOE) Apartado Postal 51 y 216, 72000, Puebla,
 Pue., Mexico

Draft version December 24, 2018

ABSTRACT

We explore the X-ray properties of a subset of the optically selected SDSS cluster sample of Goto et al. (2002), by analysing seven public XMM-*Newton* pointings, with exposure times ranging from ~ 4 to 46 ksec. There are in total 17 SDSS clusters out of which only eight are detected at X-ray wavelengths with $f_{0.5-2\text{keV}} \gtrsim 1.2 \times 10^{-14}$ ergs cm⁻² s⁻¹. For the remaining 9 SDSS clusters we estimate their 3σ luminosity upper limits (corresponding to $L_x \lesssim 5 \times 10^{42}$ ergs/sec in the 0.5-2 keV band). This relatively low luminosity suggests that if real structures, these galaxy aggregations correspond to poor groups of galaxies. Using the SDSS photometric catalogue we also derive the cluster optical r -band luminosities. The resulting scaling relations ($L_{\text{opt}} - L_x$, $L_{\text{opt}} - T_x$) are consistent with those of other recent studies.

Subject headings: galaxies: clusters: X-rays, general - large-scale structure of universe

1. INTRODUCTION

The intense recent interest on galaxy cluster studies is based on the tight cosmological constraints that they can provide, not only from their large-scale distribution, baryon fraction, clustering and dynamics, but lately also from their internal dynamics, its evolution and non-linear physical processes, that give rise in a variety of phenomena related to their formation processes (eg. Peebles et al. 1989; Borgani & Guzzo 2001; Rosati, Borgani & Norman 2002). However, in order for such studies to provide the tight constraints on cosmological parameters, that we have recently seen from the amazing CMB experiments (cf. BOOMERANG, ARCEOPS, WMAP etc) it is essential to understand and eliminate all possible systematic biases that enter in the construction and identification procedures of cluster samples (eg. Nichol 2002).

To this end a large effort has recently been put forward to construct large, bias-free, samples of clusters of galaxies spanning a wide redshift range (eg. Postman et al. 1996; Olsen et al. 1999; Gladders & Yee 2000; Goto et al. 2002; Bahcall et al. 2003). A striking result emerging from such studies is that the identified clusters strongly depend not only on the detection algorithm but also on the wavelength used. Optical selection methods, based on galaxy overdensities in two-dimensions are biased due to projection effects, although more sophisticated methods, using color information and/or structural cluster features, provide a more uniform selection of clusters (cf. Postman et al 1996). However, even such algorithms may suffer from projection effects and biases towards more evolved galaxy populations. Alternatively, X-ray selected cluster samples are less prone to biases due to the centrally peaked X-ray emitting cluster core which can be seen even at large ($z \sim 1$) distances (eg. Stocke et al. 1991; Castander et al. 1995; Ebeling et al. 1996a, 1996b; Scharf et al. 1997; Ebeling et al. 2000; Böhringer et al. 2001; Gioia et al. 2001; Rosati, Borgani & Norman 2002). Nevertheless even such identification procedure could be biased towards the

most virialized (and hence more X-ray luminous) clusters. A novel cluster detection approach has recently been proposed using simultaneous multiwavelength data with the use of Virtual Observatory data (Schuecker et al. 2004). A generic problem, however, arises from our ignorance of the cluster formation and evolution details which further complicates the characterization of clusters found at high redshifts and their use as cosmological probes.

Attempts to understand the systematic biases that enter in cluster selection procedures have been recently presented in the literature (cf. Donahue et al 2002; Basilakos et al 2004 and references therein). This letter further contributes to this issue by investigating the X-ray properties of a subsample of the Goto et al (2002) clusters detected in the SLOAN DIGITAL SKY SURVEY (SDSS) with the Cut and Enhance method (CE), which is based on galaxy colors¹. We correlate the positions of these CE cluster candidates with the extended X-ray source position, in order to investigate which of the clusters show significant X-ray emission, and thus have a larger probability of being true aggregations of galaxies. Throughout this paper we adopt the concordance cosmological model ($\Omega_m = 1 - \Omega_\Lambda = 0.3$), although all relevant quantities are parametrized according to $H_0 = 100 h$ km s⁻¹Mpc⁻¹, in order to facilitate comparisons with other studies.

2. XMM-NEWTON DATA ANALYSIS

We use XMM-*Newton* archival observations, with a proprietary period that expired before September 2003, that overlap with the first data release of the SDSS (DR1; Stoughton et al. 2002). Only observations that use the EPIC (European Photon Imaging Camera; Strüder et al. 2001; Turner et al. 2001) cameras as the prime instrument operated in full frame mode were employed. For fields observed more than once with the XMM-*Newton* we use the deeper of the multiple observations. A total of 7 fields are used with Galactic N_H in the range $2 - 8 \times 10^{20}$ cm⁻² and PN good time intervals between 4 and 46 ksec (see Table

¹ The CE catalogue is available from T.Goto, but it can also be found in <http://www.astro.noa.gr/xray/data/catalogues.html>

1). Note that two of the fields have clusters as prime targets (Abell 267 and RX J0256.5+0006). The X-ray data reduction, source detection and flux estimation are carried out using methods described in Georgakakis et al. (2004).

In total there are 17 CE optical cluster candidates in the region covered by the analyzed XMM-*Newton* observations (see Table 2). We search for extended X-ray sources around the 17 CE clusters, in the 0.5-2 keV merged PN+MOS images, where available, using the *emldetect* task of SAS. We find that extended sources are associated with 8 out of the 17 clusters (note that two of these 8 clusters were the prime targets of two of the XMM-*Newton* pointings). These were visually inspected to exclude the possibility of spurious detections due to their possible association with the CCD gaps, hot pixels or the field of view edges. Two examples of poor clusters (No 2 and 16 of Table 2) are shown in Figure 1, where the SDSS *r*-band image is overlaid with the X-ray contours.

Note that 3 out of the 17 CE optical clusters are also found in the Bahcall et al. (2003) cluster candidate list, which is based on the joint application of two different algorithms on the SDSS photometric galaxy data, while it contains 2 more clusters not found in Goto et al. Out of the 3 common clusters, two are detected in X-ray's (No.5 and No.13 of our Table 2).

For each cluster candidate we estimate the X-ray flux from a region which encompasses all the extended emission. Then we correct to the total flux by integrating a King profile to infinity: $l_x \propto [1 + (r/r_c)^2]^{-3\beta+1/2}$, where β is the ratio of energy per unit mass in galaxies to that in gas. We fix the exponent of the profile to $\beta = 0.5$ and the core radius to 100 kpc for clusters with (uncorrected) luminosities $L_x \leq 10^{43} h^{-2}$ ergs/sec and 200 kpc for those with $L_x > 10^{43} h^{-2}$ ergs/sec. We find that varying the core radius by ± 50 kpc changes the total flux by ~ 8 per cent. The conversion from count rates to flux is performed assuming a Raymond-Smith (RS) spectrum with the temperature derived from the spectral fit (see below). For the clusters that have not been detected we have estimated their 3σ upper limits, by extracting the counts in a 1 arcmin circle around the cluster optical center. Background counts were estimated from nearby regions. Then count rate upper limits are evaluated using the method described in Kraft et al. (1991). We convert the count rates to flux assuming a RS spectrum with a temperature of 2 keV, typical of poor clusters of galaxies. The total flux is estimated using the King profile above.

We investigate the X-ray spectral properties of the eight detected clusters by performing individual spectral fittings using the XSPEC v11.2 package. For four clusters which have enough photon statistics (5, 11, 16, 17) we have used the standard χ^2 analysis. For the other four we use the C-statistic instead (Cash 1979) which is proper for fitting spectra with a limited number of counts. We fit simultaneously the PN and MOS data in the energy range 0.3-8 keV. We use a RS spectrum with the abundance fixed at $Z = 0.3$, absorbed by the Galactic hydrogen column density listed in Table 1.

Finally we present in Table 2 the optical and X-ray properties for our clusters. Specifically, we list their optical equatorial coordinates (J2000), the detected flux (bold) or the 3σ upper flux limits in units of 10^{-14} erg $\text{cm}^{-2} \text{s}^{-1}$, the

cluster redshift (spectroscopic or photometric estimated by the CE method), optical *r*-band luminosities (see next section), X-ray luminosities (erg s^{-1}) in the 0.5-2 keV band, best-fit temperatures and χ^2 values, where available, of the spectral fits.

It is interesting that the majority of the CE optical cluster candidates are not identified in X-rays which could be either because they are poor, dynamically young, systems which have very low X-ray emission, or the result of projection effects. The 3σ upper X-ray luminosity limits are low, for most cases $L_{0.5-2\text{keV}} < 3 \times 10^{42} h^{-2} \text{ erg s}^{-1}$, corresponding to the emission of poor groups of galaxies. In order to investigate this issue we determine the optical properties of all 17 CE cluster candidates.

3. OPTICAL SDSS DATA ANALYSIS

We estimate the optical luminosity of the cluster candidates by cross-correlating the cluster positions with the SDSS photometric *r*-band galaxy survey. For each cluster we select all galaxies with $m_r \leq 21$ (a limit to which there is excellent star-galaxy separation) falling within a distance of $0.5 h^{-1}$ Mpc from the cluster center (for the cases where no spectroscopic redshift was available we used the estimated Goto et al. photometric redshift). However, the cluster galaxy membership is affected by foreground/background contamination and therefore we estimate the local background by using a circular area of a 1.5 degrees radius around each cluster center. We first exclude the high surface density regions and then measure the background surface density, σ_b . The background galaxy counts, projected on the surface covered by each cluster at its rest-frame, are estimated by: $N_{\text{back}} = \pi d^2 \sigma_b$, where d is the angular cluster radius corresponding to $0.5 h^{-1}$ Mpc at the cluster rest-frame. Then the predicted number of the real members for each particular SDSS cluster is found by:

$$N_r = N_{\text{obs}} - N_{\text{bac}}. \quad (1)$$

We assume that for each cluster the luminosity function of galaxies can be described by a double Schechter function (eg. Smith et al. 1997), ie., $\Phi(L) = \phi_* [f_1(L) + 2f_2(L)]$, with

$$f_i(L) = \frac{1}{L_{*,i}} \left(\frac{L}{L_{*,i}} \right)^{\alpha_i} \exp \left(-\frac{L}{L_{*,i}} \right) \quad i = 1, 2 \quad (2)$$

where $L_{*,1} \simeq 3.21 \times 10^{11} h^{-2} L_\odot$ with $\alpha_1 \simeq -1.0$ and $L_{*,2} \simeq 2.02 \times 10^{10} h^{-2} L_\odot$ with $\alpha_2 \simeq -1.7$, respectively. Thus, the number of cluster galaxy members N_r can also be written:

$$N_r = V_{\text{clus}} \int_{L_{\text{min}}(r)}^{\infty} \Phi(L) dL, \quad (3)$$

where $L_{\text{min}}(r)$ is the minimum luminosity of a galaxy at distance r (corresponding to the flux limit), $r(z)$ is the luminosity distance and V_{clus} is the volume occupied by the cluster.

From eq.(1) and eq.(3) we can determine for each cluster the unknown value of normalization constant ϕ_* and thus obtain the total cluster luminosity by: $L_{\text{opt}} = V_{\text{clus}} \int_{L_{\text{min}}(r)}^{\infty} L \Phi(L) dL$. Combining the above system of equations we obtain the final expression for L_{opt} :

$$L_{\text{opt}} = N_r \frac{\int_{L_{\text{min}}(r)}^{\infty} L [f_1(L) + 2f_2(L)] dL}{\int_{L_{\text{min}}(r)}^{\infty} [f_1(L) + 2f_2(L)] dL}. \quad (4)$$

The optical cluster luminosities and their 2σ Poisson uncertainties are presented in Table 2. We find that one cluster, also undetected in X-rays, has a negative N_r value and is therefore suspect of being a fluke.

Under the assumption that both, cluster gas and galaxies are in hydrostatic equilibrium with the underline gravitational potential and also that the clusters have an approximately constant M/L , one expects power-law scaling relations between L_{opt} , L_x and T_x . Although our sample is quite small we present as an example in Figure 2 the $L_{\text{opt}} - L_x$ relation and the best fit log-log relation (solid line). The dashed lines encompass the corresponding Popescu et al. (2004) relation. The cluster detections are shown as solid points and those with only upper limits in L_x are shown as vectors, while we also plot their 2σ L_{opt} uncertainties. Note that the cluster with the highest 3σ upper L_x limit (No 8 in Table 2) is located on the XMM-Newton pointing with the lowest exposure time (3.8 ksec) and thus we are unable to provide tight constraints on its X-ray properties.

Performing a linear regression in log-log space between the different observational quantities we find the following relations: $L_{\text{opt}}/L_{\odot} = 10^{11.60(\pm 0.10)} L_x^{0.43(\pm 0.13)}$ and $L_{\text{opt}}/L_{\odot} = 10^{10.80(\pm 0.15)} T_x^{1.00(\pm 0.31)}$, with excellent fits ($\chi^2_{\nu} \simeq 0.97$ and 0.7 respectively). The above fits are in good agreement (within the 1σ errors) with the Popescu et al (2004) relations, derived from a cross-correlation of the RASS and the SDSS (114 clusters). Furthermore, they are in relatively good agreement with the theoretical expectations for virialized structures ($L_{\text{opt}} \propto L_x^{0.5}$ and $L_{\text{opt}} \propto T_x^{1.5}$).

4. CONCLUSIONS

In order to investigate the X-ray emission of the Goto et al. (2002) SDSS clusters, we have analysed seven public XMM-Newton pointings with exposure times ranging from 4 to 46 ksecs. Out of the 17 such SDSS clusters, found in the regions covered by these XMM-Newton pointings, only eight ($\sim 47\%$) are found to have extended X-ray emission with limiting flux $f_x \sim 1.2 \times 10^{-14}$ ergs cm $^{-2}$ s $^{-1}$. Note that two of these eight SDSS clusters, which are also the most X-ray luminous ones, were the prime targets of two of the XMM-Newton observations analysed. The remaining 9 clusters are probably either very poor and/or dynamically young clusters with weak X-ray emission or the results of projection effects. The derived $L_{\text{opt}} - L_x$ and $L_{\text{opt}} - T_x$ relations, using the clusters with detected X-ray emission, are consistent with those of other recent determinations.

The present work provides a first glimpse of the observations that the future DUO X-ray mission will perform. It will survey a wide angle (6000 sq. deg) in the 0.3-10 keV energy band with the aim of using ~ 10000 clusters to map the geometry of the Universe and determine with high precision its Dark Energy component. DUO will target areas covered by the SDSS in order to facilitate the cluster redshift determination. Our work helps to determine the X-ray flux depth required to identify a significant fraction of the optically selected cluster population.

This research was jointly funded by the European Union and the Greek Government in the framework of the project 'X-ray Astrophysics with ESA's mission XMM-Newton' within the program 'Promotion of Excellence in Technological Development and Research' and by the Greek-British scientific bilateral program (2002-2003) entitled "Observations of clusters and groups of galaxies with XMM-Newton". We thank the XMM-Newton science archive for the provision of the X-ray data used.

REFERENCES

- Bahcall, N.A., et al., 2003, ApJS, 148, 233
 Basilakos, S., Plionis, M., Georgakakis, A., Georgantopoulos, I., Gaga, T., Kolokotronis, V., Stewart, G.C., 2004, MNRAS, 351, 989
 Borgani, S., & Guzzo, L., 2001, Nature, 409, 39
 Böhringer H., et al., 2001, A&A, 369, 826
 Cash, W., 1979, ApJ, 228, 939
 Castander, F.J., et al., 1995, Nature, 377, 39
 Donahue, M., et al., 2002, ApJ, 569, 689
 Ebeling, H., et al., 1996a, Proc. Roentgenstrahlung from the Universe, MPE, Report 263, ed. H. U. Zimmermann, J. Trümper, H. Yorke (ISSN 0178-1719), 579
 Ebeling, H., Voges, W., Böhringer H., Edge, A.C., Huchra, J.P., Briel, U.G., 1996B, MNRAS, 281, 799
 Ebeling, H., et al., 2000, ApJ, 534, 133
 Georgakakis, A., et al. 2004, MNRAS, 349, 135
 Gioia, I. M., Henry, J. P., Mullis, C. R., Voges, M., Briel, U. G., Böhringer H., Huchra, J. P., 2001, ApJ, 553, L105
 Gladders, M. D., & Yee, H. K. C., 2000, AJ, 120, 2148
 Goto, T., et al., 2002, AJ, 123, 1807
 Kraft, R.P., Burrows, D.N., Nousek, J.A., 1991, ApJ, 374, 344
 Nichol, R. C., 2002, in ASP Conf. Ser., Tracing Cosmic Evolution with Galaxy Clusters, ed. S. Borgani, M. Mezzetti, R. Valdarnini, 268, 57
 Olsen, L. F., et al., 1999, A&A, 345, 681
 Peebles, P.J.E., Daly, R.A. & Juszkwicz, R., 1989, ApJ, 347, 563
 Postman, M., Lubin, L. M., Gunn, J. E., Oke, J. B., Hoessel, J. G., Schneider, D. P., Christensen, J. A., 1996, AJ, 111, 615
 Rosati, P., Borgani, S. & Norman, C., 2002, ARA&A, 143, 9
 Scharf, C. A., Jones, L. R., Ebeling, H., Perlman, E., Malkan, M., Wegner, G., 1997, ApJ, 477, 79
 Schuecker, P., Böhringer, H., Voges, W., 2004, AA, 420, 61
 Smith, R.M., Driver, S.P., Phillips, S., 1997, MNRAS, 287, 415
 Stocke, J. T., Morris, S. L., Gioia, I. M., Maccacaro, T., Schild, R., Wolter, A., Fleming, T. A., Henry, J. P., 1991, ApJS, 76, 813
 Stoughton, C., et al., 2002, AJ, 123, 485
 Strüder, L. et al. 2001, A&A, 365, L18
 Turner, M.J. et al. 2001, A&A, 365, L27

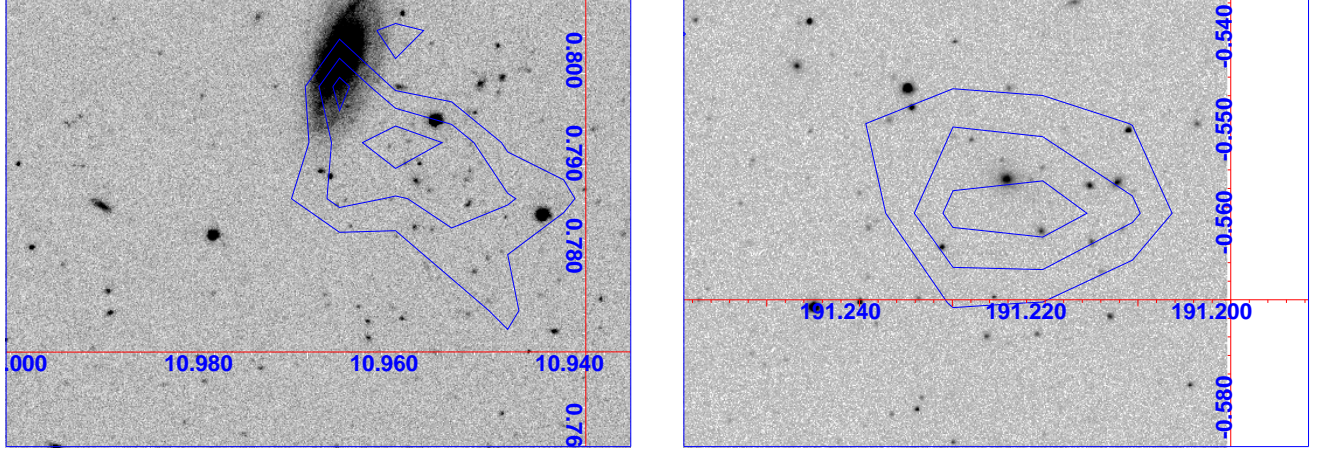


FIG. 1.— Two of the Goto et al. (2002) CE clusters detected also in X-rays. SDSS r -band images are overlaid with X-ray contours for the clusters No 2 and 16 of Table 2.

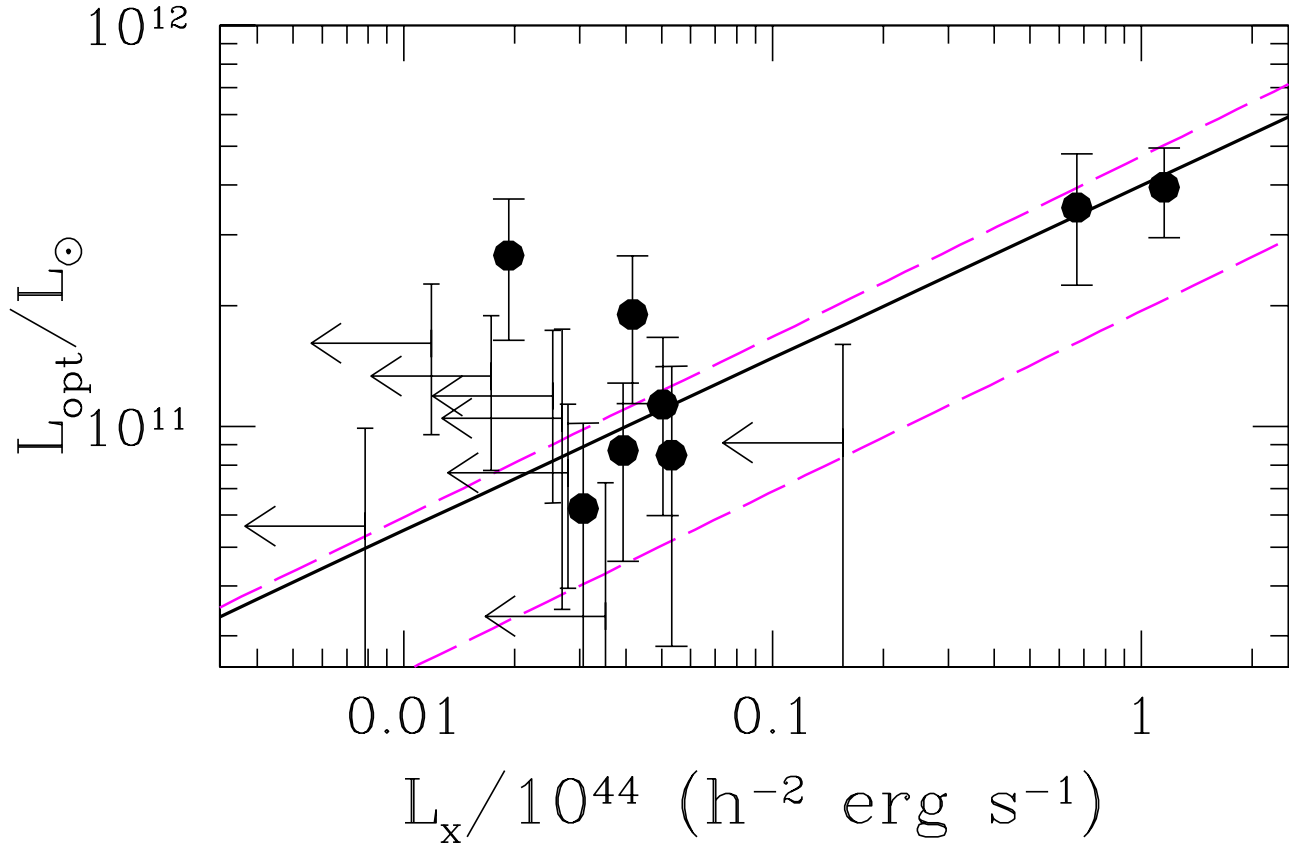


FIG. 2.— The $L_{\text{opt}} - L_x$ relation from the cluster X-ray detections. The dashed lines delineate the Popescu et al. (2004) results, while the thick continuous line corresponds to our best fit. We also show the clusters with upper L_x limits (vectors).

TABLE 1
THE ARCHIVAL XMM-*Newton* POINTINGS USED IN THIS STUDY.

RA (J2000)	Dec (J2000)	Filter	N_H (10^{20} cm^{-2})	PN exp. (sec)	MOS1 exp. (sec)	Field name	Obs. ID	P.I.
00 43 20	-00 51 15	Medium	2.33	15 700	—	UM 269	0090070201	Reeves J.
01 52 42	+01 00 43	Medium	2.80	5 800	17 200	ABELL 267	0084230401	Kneib J.P.
01 59 50	-00 23 41	Medium	2.65	3 800	—	MRK 1014	0101640201	Aschenbach B.
02 56 33	-00 06 12	Thin	6.50	—	11 600	RX J0256.5+0006	0056020301	Arnaud B.
03 02 39	+00 07 40	Thin	7.16	38 100	46 900	CFRS 3H	0041170101	Gear W.
03 38 29	+00 21 56	Thin	8.15	8 900	6 700	SDSS 033829.31+00215	0036540101	Brandt W.
12 45 09	-00 27 38	Medium	1.73	46 300	55 500	NGC 4666	0110980201	Jansen F.

TABLE 2

X-RAY FLUX UPPER LIMITS AND DETECTIONS (IN BOLD) OF THE GOTO ET AL. (2002) CE CLUSTER CANDIDATES. PHOTOMETRIC AND SPECTROSCOPIC REDSHIFTS ARE INDICATED BY THE SUPERScript 1 AND 2, RESPECTIVELY. THE SECOND COLUMN LISTS THE CORRESPONDING NUMBER OF THE BAHCALL ET AL. (2003) SDSS CLUSTERS.

#	N_{Bahcall}	α	δ	f_x	z	$L/L_\odot (\times 10^{11})$	$\log L_x$	T(keV)	χ^2_ν
1	-	10.89	1.015	8.3	0.195 ¹	0.9 ± 0.4	42.60	1.3 ^{+0.3} _{-0.2}	
2	-	10.96	0.774	3.7	0.311 ²	0.9 ± 0.6	42.72	1.4 ^{+0.5} _{-0.2}	
3	-	10.72	0.726	4.3	0.265 ²	1.9 ± 0.8	42.62	2.9 ^{+7.6} _{-1.4}	
4	173 ^a	28.05	1.108	1.7	0.243 ²	1.6 ± 0.7	42.07		
5	174	28.18	0.999	174	0.230 ¹	4.0 ± 1.0	44.06	6.9 ^{+0.3} _{-0.2}	997/768
6	-	28.18	1.138	2.7	0.219 ²	1.3 ± 0.6	42.24		
7	-	28.24	1.055	3.6	0.231 ²	1.2 ± 0.6	42.40		
8	-	29.84	0.449	2.1	0.402 ²	0.9 ± 0.7	43.19		
9	-	29.88	0.215	1.5	0.367 ²	1.1 ± 0.7	42.43		
10	-	29.88	0.283	1.8	0.356 ²	0.3 ± 0.4	42.55		
11	-	44.14	0.106	32.4	0.360 ¹	3.5 ± 1.3	43.83	5.6 ^{+0.7} _{-0.5}	202/103
12	-	45.82	-0.005	0.8	0.277 ²	0.6 ± 0.4	41.90		
13	259	54.49	0.485	1.2	0.323 ¹	2.7 ± 1.0	42.28	1.5 ^{+0.7} _{-0.6}	
14	-	54.54	0.274	6.6	0.186 ²	0.8 ± 0.4	42.45		
15	-	191.13	-0.527	0.9	0.231 ²		41.80		
16	-	191.22	-0.560	6.9	0.232 ¹	1.1 ± 0.5	42.70	1.6 ^{+0.2} _{-0.2}	128/125
17	-	191.22	-0.445	4.3	0.231 ¹	0.6 ± 0.4	42.50	1.5 ^{+0.3} _{-0.2}	168/115

^a at a distance of ~ 2.3 arcmin ($\sim 0.5 h^{-1}$ Mpc at the cluster rest-frame).